



# HHS Public Access

Author manuscript

*Biochim Biophys Acta Mol Basis Dis.* Author manuscript; available in PMC 2019 November 01.

Published in final edited form as:

*Biochim Biophys Acta Mol Basis Dis.* 2018 November ; 1864(11): 3595–3604. doi:10.1016/j.bbadis.2018.08.021.

## Reactive cysteine residues in the oxidative dimerization and Cu<sup>2+</sup> induced aggregation of human $\gamma$ D-crystallin: Implications for age-related cataract

Srinivasagan Ramkumar<sup>a</sup>, Xingjun Fan<sup>a,\*</sup>, Benlian Wang<sup>b,c</sup>, Sichun Yang<sup>c</sup>, and Vincent M. Monnier<sup>a,d,\*</sup>

<sup>a</sup>Department of Pathology, Case Western Reserve University, Cleveland, OH 44106, USA

<sup>b</sup>Center for Proteomics and Bioinformatics, Case Western Reserve University, Cleveland, OH 44106, USA

<sup>c</sup>Department of Nutrition, Case Western Reserve University, Cleveland, OH 44106, USA

<sup>d</sup>Department of Biochemistry, Case Western Reserve University, Cleveland, OH 44106, USA

### Abstract

Cysteine (Cys) residues are major causes of crystallin disulfide formation and aggregation in aging and cataractous human lenses. We recently found that disulfide linkages are highly and partly conserved in  $\beta$ - and  $\gamma$ -crystallins, respectively, in human age-related nuclear cataract and glutathione depleted LEGSKO mouse lenses, and could be mimicked by in vitro oxidation. Here we determined which Cys residues are involved in disulfide-mediated crosslinking of recombinant human  $\gamma$ D-crystallin (h $\gamma$ D). In vitro diamide oxidation revealed dimer formation by SDS-PAGE and LC-MS analysis with Cys 111–111 and C111-C19 as intermolecular disulfides and Cys 111–109 as intramolecular sites. Mutation of Cys111 to alanine completely abolished dimerization. Addition of  $\alpha$ B-crystallin was unable to protect Cys 111 from dimerization. However, Cu<sup>2+</sup>-induced h $\gamma$ D-crystallin aggregation was suppressed up to 50% and 80% by mutants C109A and C111A, respectively, as well as by total glutathionylation. In contrast to our recently published results using ICAT-labeling method, manual mining of the same database confirmed the specific involvement of Cys111 in disulfides with no free Cys111 detectable in  $\gamma$ D-crystallin from old and cataractous human lenses. Surface accessibility studies show that Cys111 in h $\gamma$ D is the most exposed Cys residue (29%), explaining thereby its high propensity toward oxidation and polymerization in the aging lens.

### Keywords

Age related cataract; Human gamma D crystalline; Cysteine disulfide; Copper oxidation

\*Corresponding authors. xing-jun.fan@case.edu (X. Fan), vmm3@case.edu (V.M. Monnier).

Appendix A. Supplementary data

Supplementary data to this article can be found online at <https://doi.org/10.1016/j.bbadis.2018.08.021>.

Transparency document

The Transparency document associated with this article can be found in online version.

## 1. Introduction

The transparency of the lens depends on a combination of homeostatic processes that minimize physical and chemical damage to crystallins, which are prone to their accumulation because they do not turn over. These include e.g. truncation, glycation, oxidation and disulfide bond formation, isomerization, racemization, deamidation, and phosphorylation [1]. Oxidation is one of the major post-translational modifications that is strongly associated with aggregation involving disulfide and non-disulfide bonds. The association between high molecular weight (HMW) aggregate and cataract is well established [2]. Oxidation extensively impacts on the sulfur-containing amino acids, cysteine and methionine [3,4]. Nuclear cataracts are associated with conformational changes and exposure of buried Cys residues thus increasing vulnerability to oxidizing species. As a result, total protein thiols decrease and protein disulfides increase [5,6]. This affects particularly the cysteine-rich  $\gamma$ -crystallins that easily form disulfide-bonded aggregates [7]. Among these, human  $\gamma$ D-crystallin is one of the most abundant and significant  $\gamma$ -crystallins of the lens nucleus [8]. One example of a critical cysteine residue is the point mutant R14C which results in hereditary juvenile cataract involving non-native cross-links with Cys 110 (now Cys111) [9].

To understand the role of cysteines in cataractogenesis, we recently determined disulfide cross-link formation sites by  $H_2O_2$  oxidation in total mouse lens homogenate compared to those found in old and cataractous human lens and glutathione depleted LEGSKO mouse lens, an animal model for age-related nuclear cataract (ARNC) [7]. Results showed that  $\beta$ -crystallin disulfide linkages are highly conserved in nuclear cataracts and LEGSKO mouse lenses and reproducible by in vitro oxidation of young mice lens by  $H_2O_2$ . However, some of the  $\gamma$ -crystallin disulfide formation sites present in human cataracts, such as 33 and 42, were not mimicked by in vitro oxidation, apparently necessitating prior conformational changes.

The study below was initiated with the goal of identifying the in vitro oxidation sites of cysteine residues in recombinant human  $\gamma$ D-crystallin. Below we report the identification of Cys 111 as the major residue responsible for disulfide formation in protein dimers as well as for  $Cu^{2+}$ -induced aggregation of h $\gamma$ D-crystallin.

## 2. Materials and methods

### 2.1. Human $\gamma$ D-crystallin and $\alpha$ B-crystallin recombinant protein expression

Human  $\gamma$ D-crystallin in the pET 3d expression vector, a kind gift from Dr. Noriko Fujii, was transformed into *E. coli* BL21 (DE3) pLysS cells. Recombinant protein was induced by isopropyl-1-thio- $\beta$ -D-galactopyranoside (IPTG) with a final concentration of 0.3 mM. The cells were collected 5h after IPTG induction, and lysed via repeated thaw and sonication cycle (six rounds of 8 pulses per minute) in 20 mM Tris-HCl, pH 8 containing 1 mM ethylenediamine tetraacetic acid (EDTA) and 1 mM phenyl methanesulfonyl fluoride (PMSF). The cell lysate was centrifuged at 20,000 $\times$  rpm for 20 min, and the supernatant was subjected to ion exchange column chromatography on a Q-Sepharose XL column (Amersham Biosciences, Piscataway, NJ) followed by a cation exchange column

chromatography on a Toyopearl GigaCap S-650M column (TOSOH, Tokyo, Japan) in a HPLC system (WATERS, Milford, MA).

Human  $\alpha$ B-crystallin construct with His-tag C-terminal was a kind gift from Dr. Mark Petrash. Recombinant  $\alpha$ B-crystallin was also produced in BL21 (DE3) pLysS *E. coli* system induced by 1 mM IPTG. The recombinant  $\alpha$ B-crystallin protein was purified via Ni-NTA affinity column (GE Health Care, Chicago, IL) following the manufacturer's protocol. The  $\alpha$ B-crystallin was eluted by 250 mM imidazole. The purity of the recombinant protein was verified by a 12% sodium dodecyl sulfate-polyacrylamide gel electrophoresis (SDS-PAGE) after Coomassie blue stain. Both purified human  $\gamma$ D and  $\alpha$ B-crystallin were dialyzed against 50 mM Chelex-treated phosphate buffer (pH 7.4) and stored in  $-80^{\circ}\text{C}$  until use.

## 2.2. In-gel digestion and mass spectrometry analysis

Human  $\gamma$ D WT and diamide oxidized (see below) crystallin samples, before cysteine alkylation was used for in-gel digestions. Briefly, samples were first separated by 12% SDS-PAGE, and the monomer and dimer band were excised and destained with 50% acetonitrile in 100 mM ammonium bicarbonate followed by 100% acetonitrile. The dehydrated gel pieces were dried in a SpeedVac centrifuge, and then digested for 5 h in 50 mM ammonium bicarbonate containing 1% (WT/WT) sequencing grade modified trypsin (Promega, Madison, WI) and then with 1% (WT/WT) Asp-N (Roche, Germany) digestion overnight digestion at  $37^{\circ}\text{C}$ . The resulting proteolytic peptides were extracted from the gel with 50% acetonitrile in 5% formic acid, the peptides were then dried and reconstituted in 0.1% formic acid for LC-MS/MS analysis.

The digests were analyzed by LC-MS/MS using Orbitrap Elite Hybrid Mass Spectrometer (Thermo Fisher Scientific, Waltham, MA), equipped with a Waters nanoAcquity UPLC system (Waters, Taunton, MA). The spectra were acquired in the positive ionization mode by data-dependent methods consisting of a full MS scan at 120,000 resolution and MS/MS scans of the twenty most abundant precursor ions in ions trap by collision-induced dissociation at normalized collision energy of 35%. A dynamic exclusion function was applied with a repeat count of 2, repeat duration of 30 s, exclusion duration of 45 s, and exclusion size list of 500. The obtained data were submitted for customized  $\gamma$ D-crystallin database search using MassMatrix [10]. Carbami-domethylation of Cys and oxidation of Met was selected as variable modifications. The mass tolerance was set as 10 ppm for precursor ions and 0.8 Da for product ions. The candidates of disulfide bonds formation suggested by the software were further verified by manual interpretation of the MS/MS spectra.

## 2.3. Site-directed mutagenesis

The  $\gamma$ D-crystallin cysteine to alanine mutants, C19A, C33A, C42A, C79A, C109A, C111A, C19-111A C19-42A, C109-111A, C19-33-42A and C19-33-42-111A, were generated by site-directed mutagenesis using the Quick Change II XL site-directed mutagenesis kit (Agilent Technologies, Santa Clara, CA) following the manufacturer's protocol. The primer pairs used for mutagenesis are listed in Table S1. All mutagenesis sites were validated by DNA sequencing analysis.

## 2.4. Human $\gamma$ D crystallin cysteine residue oxidation

Human wild type (WT) and mutant recombinant  $\gamma$ D-crystallin at the concentration of 1 mg/ml in 50 mM Chelex-treated phosphate buffer (pH 7.4) was incubated with freshly prepared 10  $\mu$ M diamide at 37 °C for 3 h. The reaction was terminated by additional 30 min incubation with 50  $\mu$ M (five equivalent) of L-cysteine to block excess unreacted diamide. The reaction mixture was concentrated using 3kDA Amicon filters, and free cysteines were alkylated with 100 mM iodoacetamide in 200 mM Tris-buffer (pH 8.5), 5 mM EDTA, 4 M urea buffer at 37 °C for 30 min. Disulfide bond formation was monitored by 12% SDS-PAGE.

In other experiments, 1:1 and 1:3 (WT/WT) mixtures of h $\gamma$ D and  $\alpha$ B crystallin in 50 mM Chelex treated potassium phosphate buffer were incubated 60 min at 37 °C and the mixture was oxidized with 10  $\mu$ M diamide and processed as described above. The formation of  $\gamma$ D-crystallin dimer was determined by 12% SDS-PAGE and also further confirmed by western blot analysis using polyclonal human  $\gamma$ D crystallin antibody (Sigma, St. Louis, MO).

## 2.5. Biophysical characterization

**2.5.1. Secondary and tertiary structure analysis**—A circular dichroism (CD) spectropolarimeter (Jasco 810, Kyoto, Japan) was used to record the CD spectra of the  $\gamma$ D crystallin and mutants. Far-ultraviolet (UV) CD measurements were performed between wavelengths of 195 to 250 nm at room temperature. Scans were performed using a cylindrical quartz cuvette with a 1 mm path length. Protein samples of 0.1 mg/ml were prepared in 50 mM potassium phosphate buffer (pH 7.4). Spectra represented are the average of five scans after subtracting blank [11].

Near-ultraviolet (UV) CD measurements were performed between wavelengths of 240 to 320 nm at room temperature. Scans were performed using a cylindrical quartz cuvette with a 10 mm path length. Protein samples of 1 mg/ml were prepared in 50 mM potassium phosphate buffer (pH 7.4). Spectra represented are the average of five scans. The buffer signal was subtracted and smoothed [12].

**2.5.2. Determination of tryptophan fluorescence**—The intrinsic tryptophan fluorescence spectra of  $\gamma$ D-crystallin mutants were recorded with an Agilent fluorescence spectrophotometer (Santa Clara, CA). The excitation was set as 295 nm and emission was recorded from 300 nm to 400 nm. Protein samples at the concentration of 0.1 mg/ml in 50 mM potassium phosphate buffer (pH 7.4) were used for the measurement as described in a previous study [11].

**2.5.3. Equilibrium unfolding**—Human  $\gamma$ D-crystallin WT and mutants (1 mg/ml) were diluted into serial concentrations of guanidinium chloride and incubated overnight at 37 °C. The intrinsic tryptophan fluorescence spectra were recorded with Tecan fluorimeter (Tecan Trading AG, Switzerland), and the ratio of fluorescence intensities at 360 and 320 nm was used as a marker of the protein folding state. These wavelengths were chosen because they represent the emission peaks of unfolded and natively folded  $\gamma$ D, respectively [13].

## 2.6. Cu<sup>2+</sup> induced aggregation assay

**2.6.1. Turbidity assay**—Human  $\gamma$ D crystallin and mutant aggregation by Cu<sup>2+</sup> was previously described [14]. Briefly, protein at the concentration of 50  $\mu$ M was incubated in 20 mM Chelex-treated potassium phosphate buffer (pH7.4) in 1, 3 and 5 equivalent of Cu<sup>2+</sup> at 37 °C for 180 min in the total volume of 200  $\mu$ l. Protein without Cu<sup>2+</sup> was used as the control. The protein mixture was incubated and analyzed using a Tecan Spectra Fluor plus 96-well plate reader (Tecan Trading AG, Switzerland). Absorbance at 405 nm [14] was monitored every 30 s, with shaking for 5 s before measurement. The turbidity assay was carried out at least six times for each condition [14].

**2.6.2. In vitro glutathionylation of  $\gamma$ D crystallin**—1 mg/ml of h $\gamma$ D-crystallin WT was incubated at 37 °C for 60 min in 50 mM potassium phosphate buffer with 1 mM GSSG [15]. Excess unreacted GSSG was removed using 10kDa centrifugal filters (Millipore, Burlington, MA). The sample was then analyzed by non-reducing SDS-PAGE and resolved protein was electroblotted onto a PVDF at 100 V for 1 h. The membrane was blocked for 1 h at room temperature in phosphate buffer saline with 0.1% Tween-20 (PBS-T) containing 5% (w/v) skimmed milk powder. After three washes with PBS-T of 5 min each, the membrane was incubated with monoclonal anti-GSH antibody (ViroGen Corp., Watertown, MA, USA) at a dilution of 1:5000 3% (w/v) BSA in PBS-T for overnight at 4 °C. After washing, the membrane was incubated for 1 h with anti-mouse immunoglobulin G (IgG) conjugated to alkaline phosphatase secondary antibody (Sigma, St. Louis, MO) at a dilution of 1:5000 in 5% (w/v) skim milk powder in PBS-T. Blots were washed as above and labeled proteins were detected with Super Signal West Pico Chemiluminescent Substrate according to the manufacturer's instructions (Thermo Fisher Scientific, Waltham, MA).

**2.6.3. Turbidity assays of glutathionylated human  $\gamma$ D-crystallin**—50  $\mu$ M of glutathionylated h $\gamma$ D crystallin WT in Chelex treated potassium phosphate buffer (pH 7.4) in 1, 3 and 5 equivalent of Cu<sup>2+</sup> and protein at 37 °C for 200 min in the total volume of 200  $\mu$ l. The protein with and without Cu<sup>2+</sup> as the negative control and unmodified  $\gamma$ D crystallin WT acted as the positive control. The protein mixtures were incubated and analyzed using a Spectra Fluor plus Tecan 96 well plate reader (Tecan Trading AG, Switzerland). Absorbance at 405 nm was monitored every 30 s, shaking 5 s before measurement. Six replicates for each experiments were performed.

## 2.7. Human lens samples for ICAT analysis

All human tissue used for this study was approved by Case Western Reserve University Institutional Review Board (IRB). Three young human eyes at the age of 3, 7 and 15 years and three normal old human eye young normal human at age of 68, 72 and 74 years were obtained from the Cleveland Eye Bank/Midwest Eye Bank within post-mortem interval of 2–8 h (average at 4.1 h). The lenses were processed for ICAT-based quantification by mass spectrometry the database of which was originally deposited into ProteomeXchange Consortium bank [17] and now mined for specific oxidation of  $\gamma$ D Cys111 residue in the particular sequence GQMIEFTEDC109SCys111LQDR. In this two-step tagging procedure, all free SH-groups are first blocked using iodoacetamide before reduction of disulfides with TCEP, and the released SH groups are then alkylated with the ICAT reagent, whereby <sup>13</sup>C vs

$^{12}\text{C}$ -ICAT reagent is used to compare e.g. old vs young, or cataractous vs. non-cataractous samples.

## 2.8. Computational docking

The 1.25-Å crystal structure of human  $\gamma$ -D crystallin (PDB entry 1HK0) was used for docking to generate its dimeric form [16]. The dimeric model with an intermolecular Cys111-Cys111 disulfide bond was generated by imposing a distance constraint with a cutoff of 5 Å between the two cysteine residues, using the protein-protein docking software ClusPro [17], where top 10 best ranking structures were selected via a Ca-RMSD clustering selection from a total of 70,000 rotations between two monomers. Local energy minimization was performed for the intermolecular Cys111-Cys111 disulfide bond before final structures models were reported.

## 2.9. Western blotting

Human WT and mutant  $\gamma$ D crystallin were separated by 12% SDS-PAGE gels, and proteins were transferred to nitrocellulose membrane at 100 V for 1 h. The membrane was blocked with 5% (w/v) skimmed milk in phosphate buffer saline with 0.1% Tween-20 (PBS-T). The membrane was then incubated with polyclonal anti- $\gamma$ D-crystallin antibody (1:5000) (Sigma St. Louis, MO) in PBS-T containing 0.1% BSA overnight at 4 °C. After washing, the membrane was incubated for 1 h at room temperature with anti-rabbit HRP conjugated secondary antibody (1:5000) (Sigma, St. Louis, MO) in 5% (w/v) skim milk PBS-T. Blots were washed and detected with chemiluminescent substrate according to the manufacturer's instructions (Thermo Fisher Scientific, Waltham, MA).

## 3. Results

### 3.1. In vitro oxidation enhances disulfide crosslinking in human $\gamma$ D crystallin

Recombinant human  $\gamma$ D crystallin (h $\gamma$ D) was incubated with 10  $\mu\text{M}$  of diamide, a mild thiol oxidizing agent, for 3h and free cysteine residues were alkylated. Analysis of the incubation mixture using 12% SDS-PAGE with a non-reduced gel and detection with either Coomassie stain or western blot revealed a new band at about 42kD corresponding to the dimeric form of h $\gamma$ D (Fig. 1A & B).

To determine the site responsible for dimer formation, the monomeric and dimeric protein bands were in-gel digested with trypsin and Asp-N enzymes and sequenced by LC-MS/MS. Results revealed the presence of a single disulfide cross-link at Cys111 (Fig. 1C).

Cys111 was also found to form cross-links with Cys19 and Cys109 (Figs. S1 & S2). A summary of disulfide forming sites is shown in Table 1. To confirm the role of these residues in disulfide formation, Cys19, 33, 42, 72, 109 and Cys111 were mutated to alanine. As shown by western blot using both a reduced and non-reduced gel, mutation to alanine did not inhibit dimer formation, except for replacing Cys111 which completely abolished dimer formation (Fig. 2). Identical results were obtained with  $\text{H}_2\text{O}_2$  (Fig. S3). However, because  $\text{H}_2\text{O}_2$  can also oxidize tryptophan [18], studies were performed with the milder oxidizing agent diamide. Note that the bands for C19A, C42A, and C79A migrate slightly but



noticeably lower than those for WT, C33A, and C109A for reasons that may involve cysteine acid formation or non-native, aggregation-prone intramolecular aggregates [19].

### 3.2. Structural and conformational stability of $\gamma$ D crystallin and cysteine mutants

The far UV-CD spectra of WT and cysteine mutants indicate the presence of wavelength minima at 217 nm that are characteristic of  $\beta$ -sheet structure. No major changes in the secondary structure were observed between cysteine mutants (Fig. S4A). Near UV-CD spectrum of h $\gamma$ D WT and cysteine mutants revealed wavelength around 260–270 nm contributed by phenylalanine and tyrosine and 280 & 290 nm contributed by tryptophan residues. Again no differences in the tertiary structure between WT and mutants were observed (Fig. S4B).

Intrinsic tryptophan fluorescence is a sensitive parameter to determine the conformational change in response to mutational and chemical stability of the protein. Human  $\gamma$ D crystallin has four tryptophan residues. Fig. S4C shows no qualitative or quantitative differences in the excitation at 295 nm and emission spectra from 300 to 400 nm of WT and mutant proteins. To determine the structural stability of  $\gamma$ D WT crystallin and cysteine mutants, chemical denaturation by GdnHCL method was applied. The equilibrium unfolding by increasing concentration of GdnHCL and intrinsic tryptophan fluorescence intensity was monitored. To determine the ratio of fluorescence emission intensities at 360 nm and 320 nm ( $I_{360}/I_{320}$ ), was plotted against increasing concentration of GdnHCL. None of the Cys > Ala mutants showed differences in resistance to chemical denaturation compared to  $\gamma$ D crystallin WT (Fig. S5). Overall, the data reveal that single site cysteine mutation does not significantly impact on the stability and structure of h $\gamma$ D, confirming that site directed mutation of the cysteine residue to alanine does not alter conformational properties of human  $\gamma$ D crystallin.

One paradox with the discovery of the critical role of CYS111 in dimerization of h $\gamma$ D, is that our recent systematic analysis of crystallin disulfides in old and cataractous human lenses failed to reveal oxidation of Cys111 [7]. To determine whether the CYS111 site of h $\gamma$ D-crystallin was possibly protected by other lens chaperone proteins such as  $\alpha$ -crystallin, co-incubations were carried out.  $\alpha$ B-crystallin is a chaperone protein that lacks cysteine residues and therefore cannot get oxidized. Thus, we treated a 1:1 and 1:3 (WT/WT) mixture of  $\gamma$ D and  $\alpha$ B human crystallin mixture with diamide. Since purified recombinant  $\alpha$ B crystallin also had a slight band appearing near 40 kDa similar to  $\gamma$ D crystallin dimer, dimer formation of  $\gamma$ D crystallin dimer was determined by western blotting using  $\gamma$ D crystallin antibody (Fig. 3). The results show only a negligible effect on  $\alpha$ B crystallin's ability to protect the CYS111 site in h $\gamma$ D from oxidation and dimerization, even at higher concentration. This apparent discrepancy from data by Kumar and Sharma [20] may relate to the fact that we assayed only dimer for formation involving exposed SH groups rather than unfolding and protein aggregation.

### 3.3. Mass spectrometric analysis of ICAT labeled human samples

In our previous study [7], we compared aged normal and aged cataractous human lenses with young normal lenses by labeling aged normal or cataractous lenses with <sup>13</sup>C (heavy) ICAT reagent and young normal lens with <sup>12</sup>C (light) ICAT reagent. Disulfide bond

formation was identified by computational search of double peaks with 9 mass ( $m/z$ ) differences. In addition, we only reported cysteine residues involved in disulfide bond formation that were present in all three samples. In one scenario, such as Cys111 in  $\gamma$ D, if it was completely oxidized no double peak was obtained leading to exclusion and missing of the data through extraction filter criteria. In order to verify whether Cys111 was indeed sensitive to oxidation, we revisited the mass spectra database and manually extracted the peptide GQMIEFT-EDC109SCys111LQDR, a theoretical tryptic peptide from  $\gamma$ D (Fig. 4). As shown in Table 2, only heavy ICAT labeling peptide was observed in the majority of lenses, no matter whether lenses were old normal or cataractous confirming thereby that most  $\gamma$ D Cys111 peptide was disulfide bonded.

### 3.4. Stability of $\gamma$ D crystallin WT and cysteine mutants toward copper oxidation

Copper is a divalent metal ion the concentration of which increases with age and in cataract lenses [21,22] suggesting a potential role in cataract formation. Data show that human  $\gamma$ D crystallin incubation with copper leads to aggregation and disulfide formation [14]. The increase of absorbance at 405 nm indicates the formation of large light scattering aggregates. Based on the work of Quintanar et al. [14], we systematically investigated the behavior of WT and mutant crystallins toward  $\text{Cu}^{2+}$  induced aggregation at 1, 3 and 5 equivalents of copper. Fig. S6 shows  $\gamma$ D crystallin WT remains clear in the absence and presence of 1 equivalent of copper but aggregates in the presence of 3 equivalent of copper as reported earlier [14]. In the presence of 5 equivalent of copper, rapid increase in  $\gamma$ D crystallin aggregate was observed that is proposed to be purely depended on metal bridged aggregates [14]. The systematic quantitative survey of mutant behavior toward  $\text{Cu}^{2+}$  mediated aggregation is shown in Fig. 5A. Cysteine to alanine mutation at Cys19, Cys33, and Cys42 has no impact on copper induced aggregation. However, replacing cysteine 109 and 111 to alanine dramatically decreased aggregation by 50% and 80%, respectively. This result underscores the importance of Cys111 in copper induced aggregation. The effects of multiple mutations are shown in Fig. 5B. Whereas cysteine mutants Cys 19–42, Cys19–33-42 behaved like  $\gamma$ D crystallin WT, multiple mutants such as Cys19–111, Cys109–111, Cys 19–33-42–111 had 70–80% decreases in aggregation confirming that Cys 111 is a major contributor in copper induced aggregation of  $\gamma$ D-crystallin. Cys19–33-42 behaved like  $\gamma$ D crystallin WT, multiple mutants such as Cys19–111, Cys109–111, Cys 19–33-42–111 had 70–80% decreases in aggregation confirming that Cys 111 is a major contributor in copper induced aggregation of  $\gamma$ D-crystallin.

### 3.5. Cysteine glutathionylation protects against copper induced aggregation of $\gamma$ D crystallin

Since coinubation with  $\alpha$ B-crystallin chaperone failed to protect Cys111 from oxidation, we investigated whether glutathionylation could protect  $\gamma$ D crystallin aggregation by copper. Recombinant  $\gamma$ D was treated for 1 h at room temperature with 1 mM GSSG according to Castellano et al. [15]. After removal of unreacted GSSG by 10kDA filtration, aliquots of the reaction mixture were analyzed by western blotting using anti-glutathione antibodies. Recombinant  $\gamma$ D crystallin was found to react with GSSG as indicated by the appearance of an immunoreactive protein band (Fig. 6A). To confirm the involvement of cysteine residues of  $\gamma$ D crystallin in copper induced aggregation, glutathionylated  $\gamma$ D crystallin was



incubated with 1, 3 and 5 equivalent of  $\text{Cu}^{2+}$  at 37 °C for 3 h. Fig. 6B results show that cysteine glutathionylation leads to complete suppression of copper induced aggregation. From this experiment it is confirmed that surface exposed cysteine of  $\gamma$ D crystallin are major contributors of copper induced aggregation.

### 3.6. Protection of $\text{Cu}^{2+}$ mediated precipitation of hgD by alpha $\alpha$ B crystallin and $\alpha$ B minichaperone

Although  $\alpha$ B crystallin failed to suppress dimerization of hgD by diamide, we wondered whether it could still suppress precipitation of hgD by  $\text{Cu}^{2+}$  as previously published by both Kumar and Sharma [20] as well as Quintanar et al. [14]. The effect was fully reproducible by both recombinant human  $\alpha$ B crystallin (Fig. 7A), a gift of Dr. M. Petrash and  $\alpha$ B crystallin minichaperone supplied by Dr. K. Sharma (Fig. 7B), except for a slightly weaker effect of the minichaperone vs. native  $\alpha$ B crystallin when tested at 5 equivalent  $\text{Cu}^{2+}$ . Assay of the supernatant for hgD dimer revealed no suppression of dimer formation (not shown), indicating a dissociation between hgD dimer formation and solubility.

## 4. Discussion

The above study is the first to demonstrate that Cys111 in recombinant h $\gamma$ D crystallins is critically involved in disulfide bond formation catalyzed by diamide as well as in the non-oxidative aggregation and precipitation by  $\text{Cu}^{2+}$ . Several authors previously observed or postulated an increased propensity of certain  $\gamma$ -crystallin residues toward disulfide bond formation, dimerization and aggregation in vitro and in cataracts (for a review see [7] and [23]). Hanson et al. reported the formation of multiple disulfides in various human gamma crystallins, but several of these are considered artefacts of sample processing [24]. Skouri-Panet reported dimerization of human and bovine  $\gamma$ S under gentle oxidation that was linked to disulfide bonds involving Cys20 [25]. Slingsby et al. observed dimerization of calf lens  $\gamma$ -crystallins treated with ascorbic acid and/or  $\text{Cu}^{2+}$  alone [26] and postulated, based on calculations of sulfhydryl exposure to solvent, the following reactivity of cysteines in h $\gamma$ D crystallins: Cys111 > Cys19 > Cys109 > Cys42, while Cys42 and Cys33 were completely inaccessible [27]. They confirmed Cys20 as the most exposed cysteine in  $\gamma$ S [27]. However, somewhat surprisingly, C19 in h $\gamma$ D was found not or minimally oxidized [7,28] despite better exposure than C109 and C42.

What is the role of Cys111 oxidation in the formation of disulfide-linked HMW polypeptides found in cataract lenses? In the fetal lens, C111 is present in SH form [28]. Surprisingly, a systematic investigation by us and Truscott et al. on disulfide forming cysteine residues in normal aged and cataractous lens [7,28] failed to identify Cys111 as being oxidized. While these authors used the N-ethylmaleimide and iodoacetamide method [28], we used the ICAT labeling method that failed to label the Cys111 residue of the reference (i.e. non-cataractous young) sample since it had been fully blocked by iodoacetic acid in the first labeling step. This led us to reinvestigate, using manual reading method, the data deposited in the ProteomeXchange Consortium bank and find that 100% disulfides were indeed detectable by ICAT reagent at Cys111 in either old or cataractous lenses. Thus

Cys111 participates in HMW protein aggregate formation and could represent the first stage from which polymeric light scattering aggregates are formed.

To provide a molecular picture of the h $\gamma$ D crystallin dimer, computational docking was carried out based on the aforementioned intermolecular diamide oxidation as reported above. The rigid docking was based on the 1.25-Å crystal structure (PDB entry 1HK0) of human  $\gamma$ -D crystalline monomer [23] given no observation here of monomer unfolding. Top structure candidates of the dimeric form were reported after a local energy minimization between the Cys111 sulfhydryl groups of intermolecular the Cys111-Cys111 disulfide bond (see Top four models in Fig. 8). These putative models vary dramatically with respect to relative orientation between two monomers; for example, compared to structure 1, structures 2 and 3 have about 90-degree internal rotation.

However, the “sandwich shaped” structure 4 is only the 4th most likely combination. Additional structural combinations are depicted in Fig. S7. As already stated above, there is no reason to believe that the Cys111-Cys111 dimer is by itself associated with a deleterious opacification process.

One important conundrum is that in contrast to cataract data no oxidation of Cys33 and Cys42 residues was observed under the above experimental conditions, while we [7] and Hains and Truscott [28] found these to be major disulfide formation sites in the human lens. Cys111 was able to form disulfides both with itself, as well as with Cys19 and Cys109, both of which are about 9–10% exposed [27]. Yet, allegedly, the distance between Cys19, Cys109 and Cys111 was not sufficient for intramolecular disulfide formation [24]. This proposition will have to be amended since there is little doubt that an intramolecular crosslink can form between Cys109 and Cys111, as found in monomeric oxidized h $\gamma$ D (Table 1).

One potential explanation for the fact that no oxidation of Cys33 and Cys42 was observed is that more dramatic oxidation conditions and protein unfolding are needed to expose these residues. Indeed, in unpublished studies, we found that the drastic oxidizing agent H<sub>2</sub>O<sub>2</sub> could achieve oxidation of other cysteine sites into disulfides (Fig. S3) and form Cys33-Cys19 and Cys33-Cys79 crosslinks besides, Cys109-Cys111 and Cys111-Cys111 (unpublished results). These findings implicate the need for drastic structural changes and exposure of these sites. Indeed Serebryany et al. [29] showed oxidation mimicking W42Q mutant was associated with the formation of disulfides between cysteines close together in sequence, particularly Cys33 and Cys42, and that disulfides stabilized a partially unfolded intermediate state of W42Q mutants prone to specific intermolecular interactions. Also Pande et al. suggested that non-solvent accessible Cys 33 in h $\gamma$ D crystallin may also be implicated in intermolecular crosslinks with Cys 14 and C110/111 in juvenile cataract caused by mutant R14C [9].

The mechanism responsible for Cu<sup>2+</sup> mediated loss of h $\gamma$ D stability and aggregation is puzzling. An oxidative mechanism is likely but may it may go beyond C111-C111 dimer formation since  $\alpha$ B crystallin was able to suppress Cu<sup>2+</sup> catalyzed insolubilization despite dimerization. Quintanar et al. [14] suggested a mechanism based on metal bridge aggregation. Our findings agree and now strongly implicate Cys111 and to some extent

Cys109 as binding sites, while cysteine mutants C19A, C33A, C42A, C19–42A and C19–33–42A were unable to suppress the aggregation, excluding thus an important of these sulfhydryls in the process. Considerable studies have proposed that  $\text{Cu}^{2+}$  in the aging lens might have deleterious effects [30–34]. Based on the above findings,  $\text{Cu}^{2+}$  may not only participate in h $\gamma$ D destabilization via binding to Cys111 and Cys109, but might also be the redox active metal that generates  $\text{OH}\cdot$  and oxidizes critical tyrosine and tryptophan residues involved in protein stability [35,36], eventually leading to exposure of Cys 19, 33 and 42 and subsequent oxidation into disulfides.

Previous Nuclear Magnetic Resonance (NMR) studies show His84, Ser85, Ser87, His88 are the most affected residue upon addition of 0.2 and 0.6 equivalent of  $\text{Cu}^{2+}$  and that the addition of 1 to 1.5 equivalent affected Cys4/42 [14]. The limitations of these NMR studies is that only non-aggregated protein can be analyzed by this instrument and that h $\gamma$ D crystallin WT starts to aggregate only at 3 equivalent copper. The previous studies used only 0.2, 0.6 and 1 to 1.5  $\text{Cu}^{2+}$  equivalents for the NMR data analysis, i.e. was far insufficient for induction of  $\gamma$ D-crystallin aggregation. Hence it is difficult to unequivocally identify the most affected amino acid residues in  $\text{Cu}^{2+}$  modified  $\gamma$ D crystallin, and the authors themselves pointed out that specific residues involved in the mechanisms of metal-induced aggregation remain to be discovered [14]. In that regard our studies unequivocally identified Cys111 followed by Cys109 as the major amino acid sites where  $\text{Cu}^{2+}$  interact, presumably leading to structural changes and intra-and intermolecular disulfides involved in high molecular weight aggregate formation.

Finally, what mechanisms has the lens developed to protect itself from physical-chemical hits to Cys111 since it is critical for protein stability especially when copper is present? The  $\alpha$ B-crystallin oligomers could form protective complexes with their  $\gamma$ D-crystallin substrates. First and foremost, one would expect chaperone activity by  $\alpha$ B to protect, as e.g. demonstrated by Horwitz who showed that  $\alpha$ -crystallin has chaperone activity that inhibits the thermally-induced aggregation of different enzymes and bovine  $\beta$ - and  $\gamma$ -crystallins [37–39]. The  $\alpha$ B-crystallin oligomers were found to form long-lived stable complexes with their  $\gamma$ D-crystallin substrates. Sampson and King showed that  $\alpha$ B crystallin suppresses partially folded  $\gamma$ D crystallin by its chaperone function and interaction with the aggregation-prone region in C-terminal of  $\gamma$ D crystallin [40].

Much to our surprise, the addition of  $\alpha$ B had at best a mild protective effect on dimerization when incubated for 1 h, i.e. conditions under which Sharma et al. found complete protection of  $\gamma$ -crystallins when incubated with alpha B [41]. For this reason we repeated the experiment using minichaperone A and B provided by Sharma et al. [20,42], but found only minor protective effect. See data in Supplemental section Fig. S3 One reason why we found no major chaperone effect might be that we assayed dimer formation rather than unfolding mediated aggregation [14]. In contrast, the powerful effect of  $\alpha$ B and its minichaperone at preventing  $\text{Cu}^{2+}$  mediated insolubilization, as previously reported [20], may mean the minichaperone either binds and protects unfolded h $\gamma$ D, or it acts by chelating  $\text{Cu}^{2+}$ . Whatever the mechanism by which copper induces insolubilization, it must involve residues C111 and C109 together with an oxidative process since the redox inactive  $\text{Zn}^{2+}$  is considerably less active than  $\text{Cu}^{2+}$  in h $\gamma$ D precipitation [17].

Interestingly, Truscott found that up to 60% of Cys111 is methylated [43], thus likely shielding it from oxidation and metal binding. Our attempts to methylate this site were unsuccessful and thus no clear answer to the above suggestion is possible. However, protection of Cys111 by glutathionylation was successful, resulting in lower disulfide bond formation and Cu<sup>2+</sup> associated aggregation and precipitation. In the end, these protective mechanisms (glutathionylation and methylation) could be a reason why human evolution has retained cysteine at position 111 of  $\gamma$ D crystallin, while, in contrast, Cys111 serine residues are present in bovine and mouse lens.

In conclusion, these studies reveal a critical role of C111 in human recombinant  $\gamma$ D crystallin dimerization and copper mediated precipitation, whereby the latter mechanisms appears to be more important in the opacification process of the gamma crystallin rich lens nucleus during aging than aggregation via dimerization with disulfide bond formation.

## Supplementary Material

Refer to Web version on PubMed Central for supplementary material.

## Acknowledgments

This work was supported by research grants from NEI 07099 (to VMM) and in part by NEI 024553 (to XF), the Case Western Reserve University Vision Science Research Center (P30 EY 11373). We thank the National Eye Institute for supporting this research. We thank Dr. Krishna Sharma for providing samples of minichaperone for  $\alpha$ A- and  $\alpha$ B-crystallin, and we thank Dr. Mark Petrash for his gift of recombinant human alpha B crystallin cDNA plasmid [44].

## Abbreviations:

<b>Cys</b>	cysteine
<b>WT</b>	wild type
<b>h<math>\gamma</math>D</b>	human gamma D crystallin
<b>HMW</b>	high molecular weight aggregate
<b>ARNC</b>	age-related nuclear cataract
<b>IPTG-isopropyl</b>	1-thio- $\beta$ -D-galactopyranoside
<b>EDTA</b>	ethylenediamine tetraacetic acid
<b>PMSF</b>	phenyl methanesulfonyl fluoride
<b>SDS-PAGE</b>	sodium dodecyl sulfate-polyacrylamide gel electrophoresis
<b>CD</b>	circular dichroism
<b>UV</b>	ultraviolet

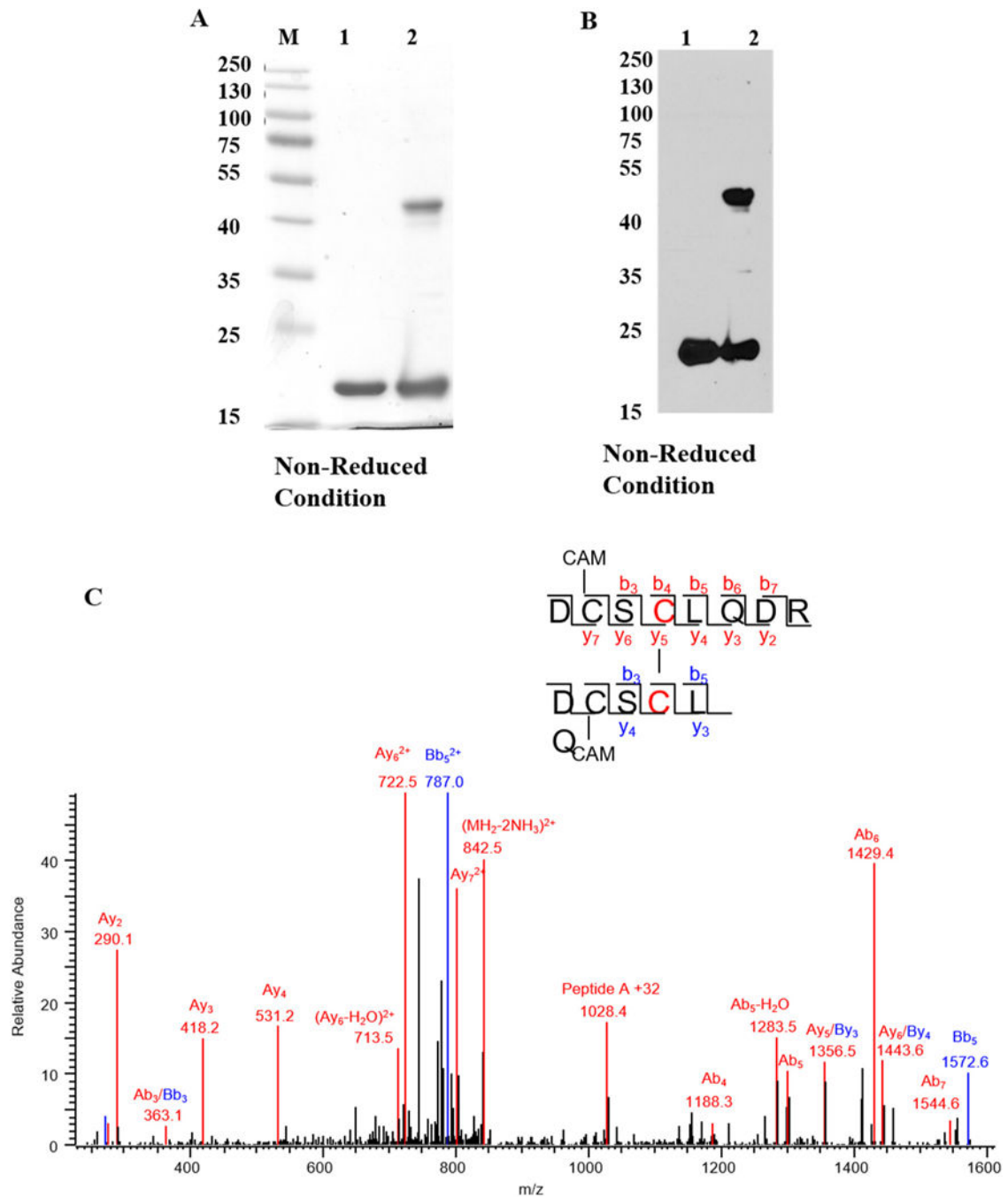
## References

- [1]. Sharma KK, Santhoshkumar P, Lens aging: effects of crystallins, *Biochim. Biophys. Acta* 1790 (2009) 1095–1108. [PubMed: 19463898]
- [2]. Jedziniak JA, Kinshita JH, Yates EM, Hocker LO, Benedek GB, On the presence and mechanism of formation of heavy molecular weight aggregates in human normal and cataractous lenses, *Exp. Eye Res.* 15 (1973) 185–192. [PubMed: 4692231]
- [3]. Truscott RJ, Augusteyn RC, Oxidative changes in human lens proteins during senile nuclear cataract formation, *Biochim. Biophys. Acta* 492 (1977) 43–52. [PubMed: 861252]
- [4]. Garner MH, Spector A, Selective oxidation of cysteine and methionine in normal and senile cataractous lenses, *Proc. Natl. Acad. Sci. U. S. A.* 77 (1980) 1274–1277. [PubMed: 6929483]
- [5]. Michael R, Bron AJ, The ageing lens and cataract: a model of normal and pathological ageing, *Philos. Trans. R. Soc. Lond. Ser. B Biol. Sci.* 366 (2011) 1278–1292. [PubMed: 21402586]
- [6]. Niwa T, Protein glutathionylation and oxidative stress, *J. Chromatogr. B Anal. Technol. Biomed. Life Sci.* 855 (2007) 59–65.
- [7]. Fan X, Zhou S, Wang B, Hom G, Guo M, Li B, Yang J, Vaysburg D, Monnier VM, Evidence of highly conserved beta-crystallin disulfidome that can be mimicked by in vitro oxidation in age-related human cataract and glutathione depleted mouse Lens, *Mol. Cell. Proteomics* 14 (2015) 3211–3223. [PubMed: 26453637]
- [8]. Vendra VP, Khan I, Chandani S, Muniyandi A, Balasubramanian D, Gamma crystallins of the human eye lens, *Biochim. Biophys. Acta* 1860 (2016) 333–343. [PubMed: 26116913]
- [9]. Pande A, Gillot D, Pande J, The cataract-associated R14C mutant of human gamma D-crystallin shows a variety of intermolecular disulfide cross-links: a Raman spectroscopic study, *Biochemistry* 48 (2009) 4937–4945. [PubMed: 19382745]
- [10]. Xu H, Zhang L, Freitas MA, Identification and characterization of disulfide bonds in proteins and peptides from tandem MS data by use of the MassMatrix MS/MS search engine, *J. Proteome Res.* 7 (2008) 138–144. [PubMed: 18072732]
- [11]. Ramkumar S, Fujii N, Sakaue H, Fujii N, Thankappan B, Kumari RP, Natarajaseenivasan K, Anbarasu K, Real-time heterogeneous protein-protein interaction between alphaA-crystallin N-terminal mutants and alphaB-crystallin using quartz crystal microbalance (QCM), *Amino Acids* 47 (2015) 1035–1043. [PubMed: 25694240]
- [12]. Nagaraj RH, Nahomi RB, Shanthakumar S, Linetsky M, Padmanabha S, Pasupuleti N, Wang B, Santhoshkumar P, Panda AK, Biswas A, Acetylation of alphaA-crystallin in the human lens: effects on structure and chaperone function, *Biochim. Biophys. Acta* 1822 (2012) 120–129. [PubMed: 22120592]
- [13]. Kosinski-Collins MS, King J, In vitro unfolding, refolding, and polymerization of human gammaD crystallin, a protein involved in cataract formation, *Protein Sci.* 12 (2003) 480–490. [PubMed: 12592018]
- [14]. Quintanar L, Dominguez-Calva JA, Serebryany E, Rivillas-Acevedo L, Haase-Pettingell C, Amero C, King JA, Copper and zinc ions specifically promote non-amyloid aggregation of the highly stable human gamma-D crystallin, *AC S Chem. Biol.* 11 (2016) 263–272.
- [15]. Castellano I, Ruocco MR, Cecere F, Di Maro A, Chambery A, Michniewicz A, Parlato G, Masullo M, De Vendittis E, Glutathionylation of the iron superoxide dismutase from the psychrophilic eubacterium *Pseudoalteromonas haloplanktis*, *Biochim. Biophys. Acta* 1784 (2008) 816–826. [PubMed: 18328273]
- [16]. Basak A, Bateman O, Slingsby C, Pande A, Asherie N, Ogun O, Benedek GB, Pande J, High-resolution X-ray crystal structures of human gammaD crystallin (1.25 Å) and the R58H mutant (1.15 Å) associated with aculeiform cataract, *J. Mol. Biol.* 328 (2003) 1137–1147. [PubMed: 12729747]
- [17]. Kozakov D, Hall DR, Xia B, Porter KA, Padhorny D, Yueh C, Beglov D, Vajda S, The ClusPro web server for protein-protein docking, *Nat. Protoc.* 12 (2017) 255–278. [PubMed: 28079879]
- [18]. Simat TJ, Steinhart H, Oxidation of free tryptophan and tryptophan residues in peptides and proteins, *J. Agric. Food Chem.* 46 (1998) 490–498. [PubMed: 10554268]

- [19]. Serebryany E, King JA, Wild-type human gammaD-crystallin promotes aggregation of its oxidation-mimicking, misfolding-prone W42Q mutant, *J. Biol. Chem.* 290 (2015) 11491–11503. [PubMed: 25787081]
- [20]. Kumar RS, Sharma KK, Chaperone-like activity of a synthetic peptide toward oxidized gamma-crystallin, *J. Pept. Res.* 56 (2000) 157–164. [PubMed: 11007272]
- [21]. Cekic O, Effect of cigarette smoking on copper, lead, and cadmium accumulation in human lens, *Br. J. Ophthalmol.* 82 (1998) 186–188. [PubMed: 9613387]
- [22]. Srivastava VK, Varshney N, Pandey DC, Role of trace elements in senile cataract, *Acta Ophthalmol.* 70 (1992) 839–841. [PubMed: 1488898]
- [23]. Fan X, Monnier VM, Whitson J, Lens glutathione homeostasis: discrepancies and gaps in knowledge standing in the way of novel therapeutic approaches, *Exp. Eye Res.* 156 (2017) 103–111. [PubMed: 27373973]
- [24]. Hanson SR, Smith DL, Smith JB, Deamidation and disulfide bonding in human lens gamma-crystallins, *Exp. Eye Res.* 67 (1998) 301–312. [PubMed: 9778411]
- [25]. Skouri-Panet F, Bonnet F, Prat K, Bateman OA, Lubsen NH, Tardieu A, Lens crystallins and oxidation: the special case of gammaS, *Biophys. Chem.* 89 (2001) 65–76. [PubMed: 11246746]
- [26]. Atalay A, Ogus A, Bateman O, Slingsby C, Vitamin C induced oxidation of eye lens gamma crystallins, *Biochimie* 80 (1998) 283–288. [PubMed: 9672746]
- [27]. Srikanthan D, Bateman OA, Purkiss AG, Slingsby C, Sulfur in human crystallins, *Exp. Eye Res.* 79 (2004) 823–831. [PubMed: 15642319]
- [28]. Hains PG, Truscott RJ, Proteomic analysis of the oxidation of cysteine residues in human age-related nuclear cataract lenses, *Biochim. Biophys. Acta* 1784 (2008) 1959–1964. [PubMed: 18761110]
- [29]. Serebryany E, Woodard JC, Adkar BV, Shabab M, King JA, Shakhnovich EI, An internal disulfide locks a Misfolded aggregation-prone intermediate in cataract-linked mutants of human gammaD-Crystallin, *J. Biol. Chem.* 291 (2016) 19172–19183. [PubMed: 27417136]
- [30]. Harris ED, Basic and clinical aspects of copper, *Crit. Rev. Clin. Lab. Sci.* 40 (2003) 547–586. [PubMed: 14653357]
- [31]. Racz P, Erdohelyi A, Cadmium, lead and copper concentrations in normal and senile cataractous human lenses, *Ophthalmic Res.* 20 (1988) 10–13. [PubMed: 3380522]
- [32]. Stanojevic-Paovic A, Hristic V, Cuperlovic M, Jovanovic S, Krsmanovic J, Macro- and microelements in the cataractous eye lens, *Ophthalmic Res.* 19 (1987) 230–234. [PubMed: 3696699]
- [33]. Rasi V, Costantini S, Moramarco A, Giordano R, Giustolisi R, Balacco Gabrieli C, Inorganic element concentrations in cataractous human lenses, *Ann. Ophthalmol.* 24 (1992) 459–464. [PubMed: 1485742]
- [34]. Khan MM, Martell AE, Metal ion and metal chelate catalyzed oxidation of ascorbic acid by molecular oxygen. II. Cupric and ferric chelate catalyzed oxidation, *J. Am. Chem. Soc.* 89 (1967) 7104–7111. [PubMed: 6064355]
- [35]. Schafheimer N, Wang Z, Schey K, King J, Tyrosine/cysteine cluster sensitizing human gammaD-crystallin to ultraviolet radiation-induced photoaggregation in vitro, *Biochemistry* 53 (2014) 979–990. [PubMed: 24410332]
- [36]. Xia Z, Yang Z, Huynh T, King JA, Zhou R, UV-radiation induced disruption of dry-cavities in human gammaD-crystallin results in decreased stability and faster unfolding, *Sci. Rep.* 3 (2013) 1560. [PubMed: 23532089]
- [37]. Horwitz J, Alpha-crystallin, *Exp. Eye Res.* 76 (2003) 145–153. [PubMed: 12565801]
- [38]. Horwitz J, Alpha-crystallin can function as a molecular chaperone, *Proc. Natl. Acad. Sci. U. S. A.* 89 (1992) 10449–10453. [PubMed: 1438232]
- [39]. Horwitz J, Bova MP, Ding LL, Haley DA, Stewart PL, Lens alpha-crystallin: function and structure, *Eye (Lond)* 13 (Pt 3b) (1999) 403–408. [PubMed: 10627817]
- [40]. Acosta-Sampson L, King J, Partially folded aggregation intermediates of human gammaD-, gammaC-, and gammaS-crystallin are recognized and bound by human alphaB-crystallin chaperone, *J. Mol. Biol.* 401 (2010) 134–152. [PubMed: 20621668]

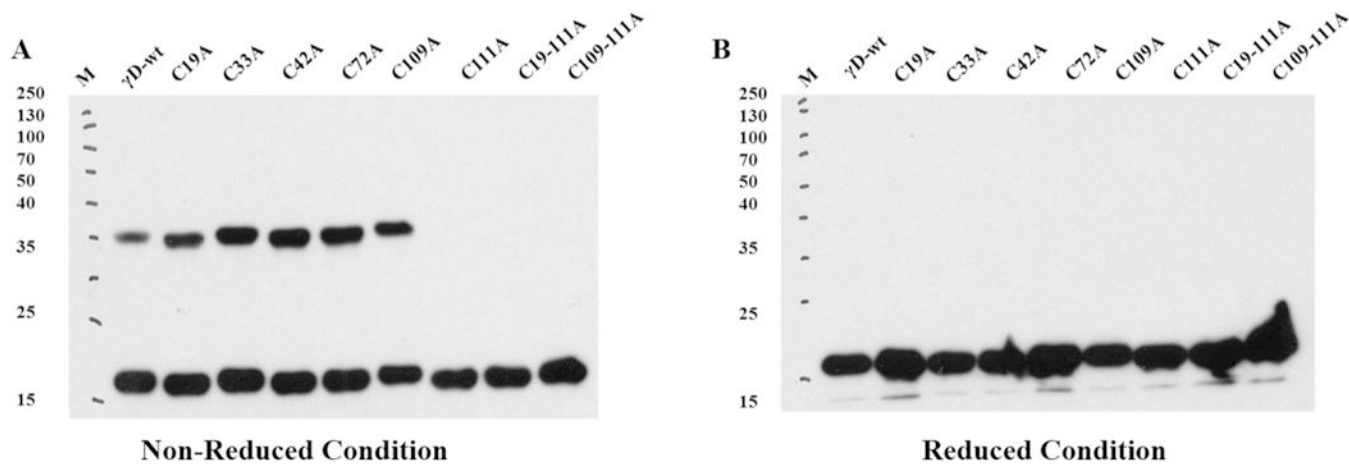


- [41]. Santhoshkumar P, Udupa P, Murugesan R, Sharma KK, Significance of interactions of low molecular weight crystallin fragments in lens aging and cataract formation, *J. Biol. Chem.* 283 (2008) 8477–8485. [PubMed: 18227073]
- [42]. Bhattacharyya J, Padmanabha Udupa EG, Wang J, Sharma KK, Mini-alphaB-crystallin: a functional element of alphaB-crystallin with chaperone-like activity, *Biochemistry* 45 (2006) 3069–3076. [PubMed: 16503662]
- [43]. Truscott RJ, Mizdrak J, Friedrich MG, Hooi MY, Lyons B, Jamie JF, Davies MJ, Wilmarth PA, David LL, Is protein methylation in the human lens a result of non-enzymatic methylation by S-adenosylmethionine? *Exp. Eye Res.* 99 (2012) 48–54. [PubMed: 22542751]
- [44]. Cobb BA, Petrash JM, Characterization of alpha-crystallin-plasma membrane binding, *J. Biol. Chem.* 275 (2000) 6664–6672. [PubMed: 10692476]

**Fig. 1.**

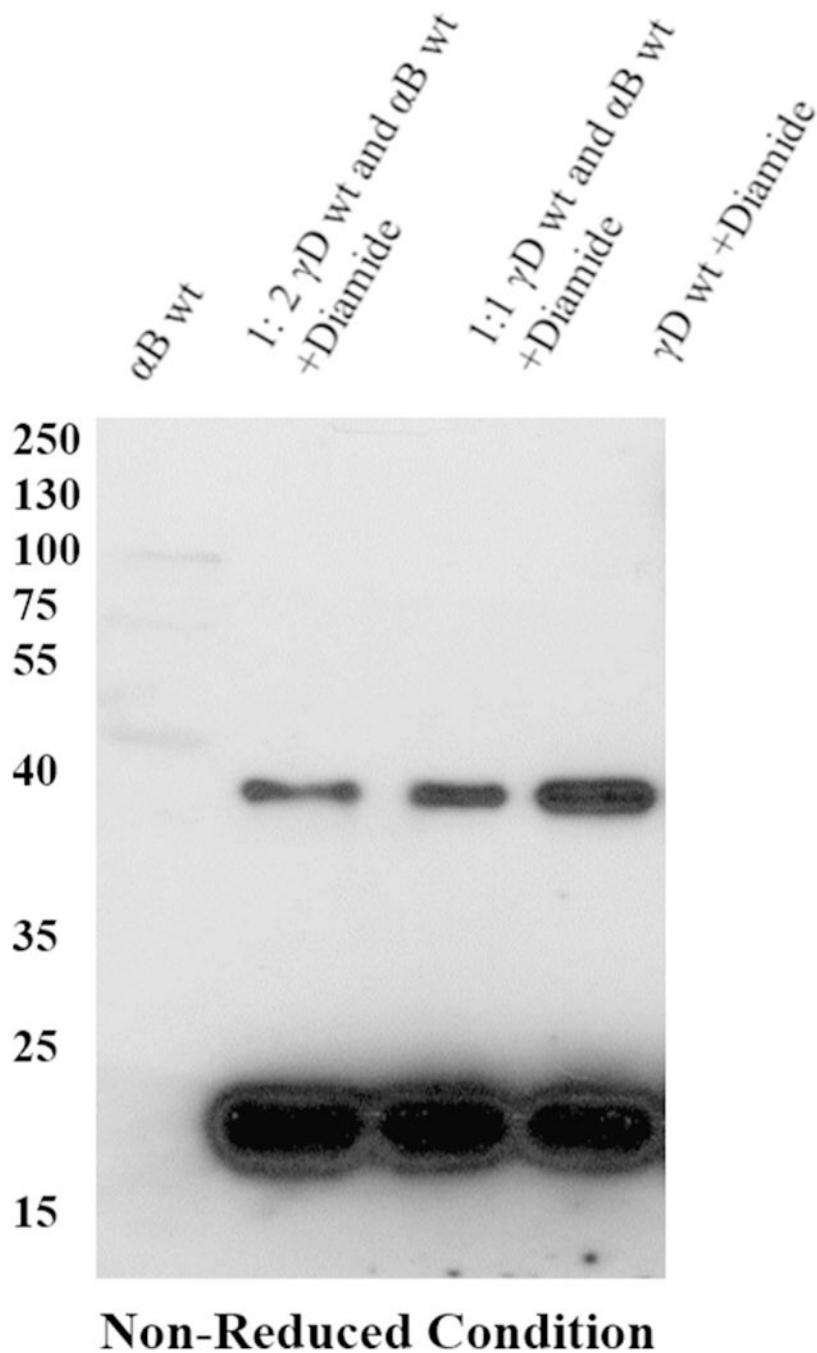
Diamide oxidation of human  $\gamma$ D-crystallin. (A) 1 mg/ml of recombinant h $\gamma$ D in Chelex treated 50mMK + /PO<sub>4</sub> buffer pH 7.4 was incubated with 10  $\mu$ l diamide at 37 °C for 3 h. Dimer formation was analyzed by 12% SDS-PAGE and destained overnight. The image was scanned under greyscale using Epson scanner. M-Protein marker, lane 1 -non-oxidized h $\gamma$ D, lane 2 -oxidized h $\gamma$ D. (B) Dimerization was confirmed by western blot using h $\gamma$ D polyclonal antibody and the blot was developed using X-ray film using ECL solution the developed film was scanned under greyscale using EPSON scanner, lane 1 -non-oxidized

h $\gamma$ D, lane 2 -oxidized h $\gamma$ D. For both SDS-PAGE and western blot samples were derived from the same experiment and processed in parallel. (C) Tandem mass spectrum of disulfide formation between Cys111-Cys111 in h $\gamma$ D dimer. Both Cys 109 residues are carbamidomethylated. The series b and y ions with A and B represent the fragment ion from peptide DCSCQLQDR (A) and DCSCQLQ (B), respectively. The precursor ion m/z is 859.8151 (2+).

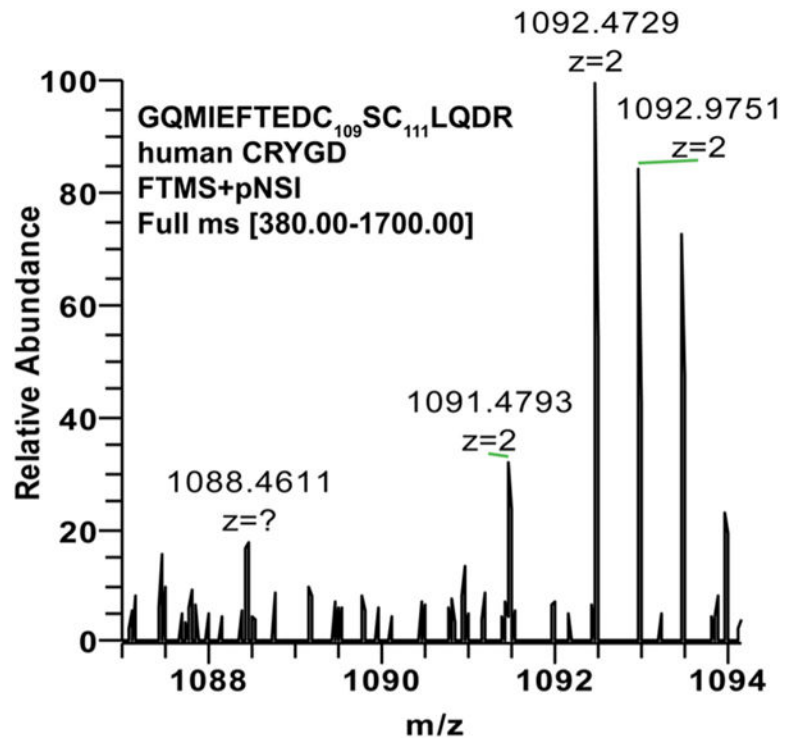


**Fig. 2.**

Western blot of dimer formation by diamide oxidation of recombinant  $\gamma$ D-crystallin and cysteine mutants in Chelex treated 50 mM potassium phosphate (pH 7.4). Protein was incubated with 10  $\mu$ M of diamide at 37  $^{\circ}$ C for 3h and disulfide bond formation was analyzed by western blot using h $\gamma$ D polyclonal antibody and the blot was developed using X-ray film using ECL solution the developed film was scanned under greyscale using Epson scanner. For both reduced and non-reduced blot samples were derived from the same experiment and blots were processed in parallel.

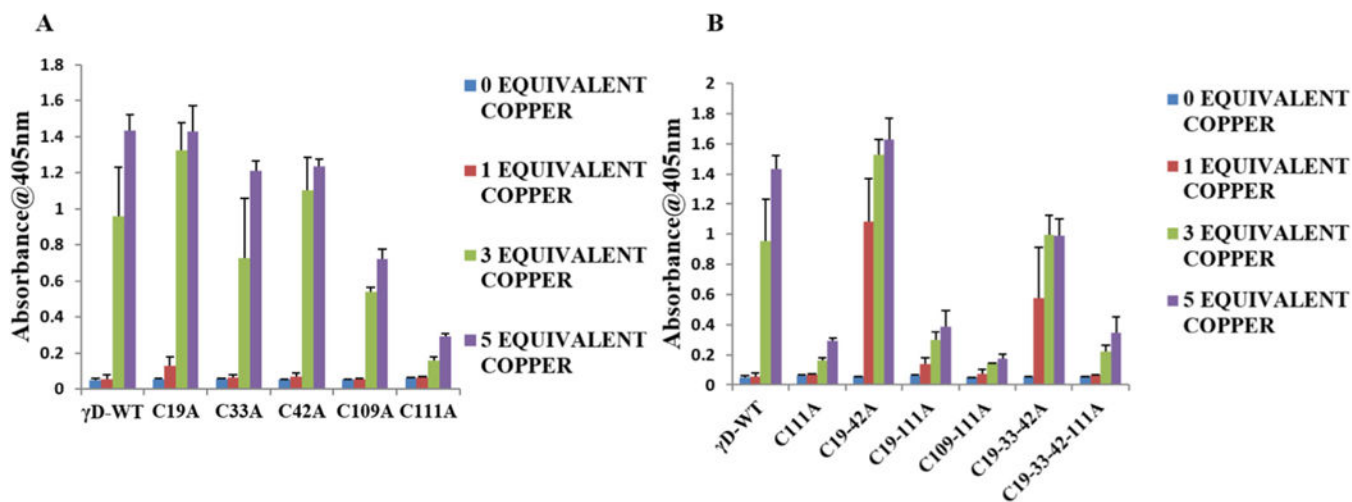


**Fig. 3.** Western blot analysis of  $\gamma$ D crystallin oxidized in the presence of  $\alpha$ B crystallin. Human  $\gamma$ D crystallin and  $\alpha$ B crystallin in the ratio of 1:1 and 1:2 were incubated 60 min at 37 °C and mixture was oxidized by diamide. The formation of dimer by  $\gamma$ D crystallin was determined by western blot analysis using  $\gamma$ D crystallin polyclonal antibody and the blot was developed using X-ray film using ECL solution the developed film was scanned under greyscale using Epson scanner.

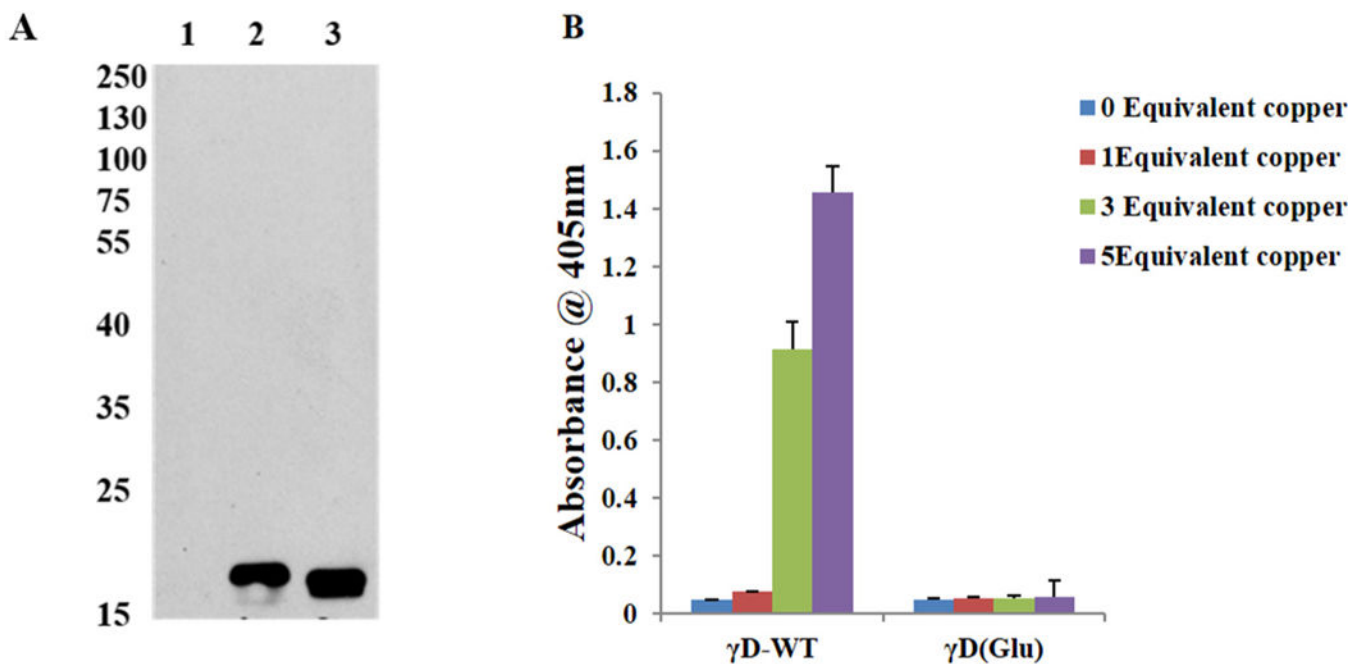


**Fig. 4.** Typical mass spectrum and analysis of individual cysteine residues involved in disulfide formation. The peptide AEFSGECSNLADR from human gamma D crystallin covering cysteine residue 111 was analyzed in human cataract level V lens nucleus using data deposited into the ProteomeXchange Consortium bank from a previous study [7].

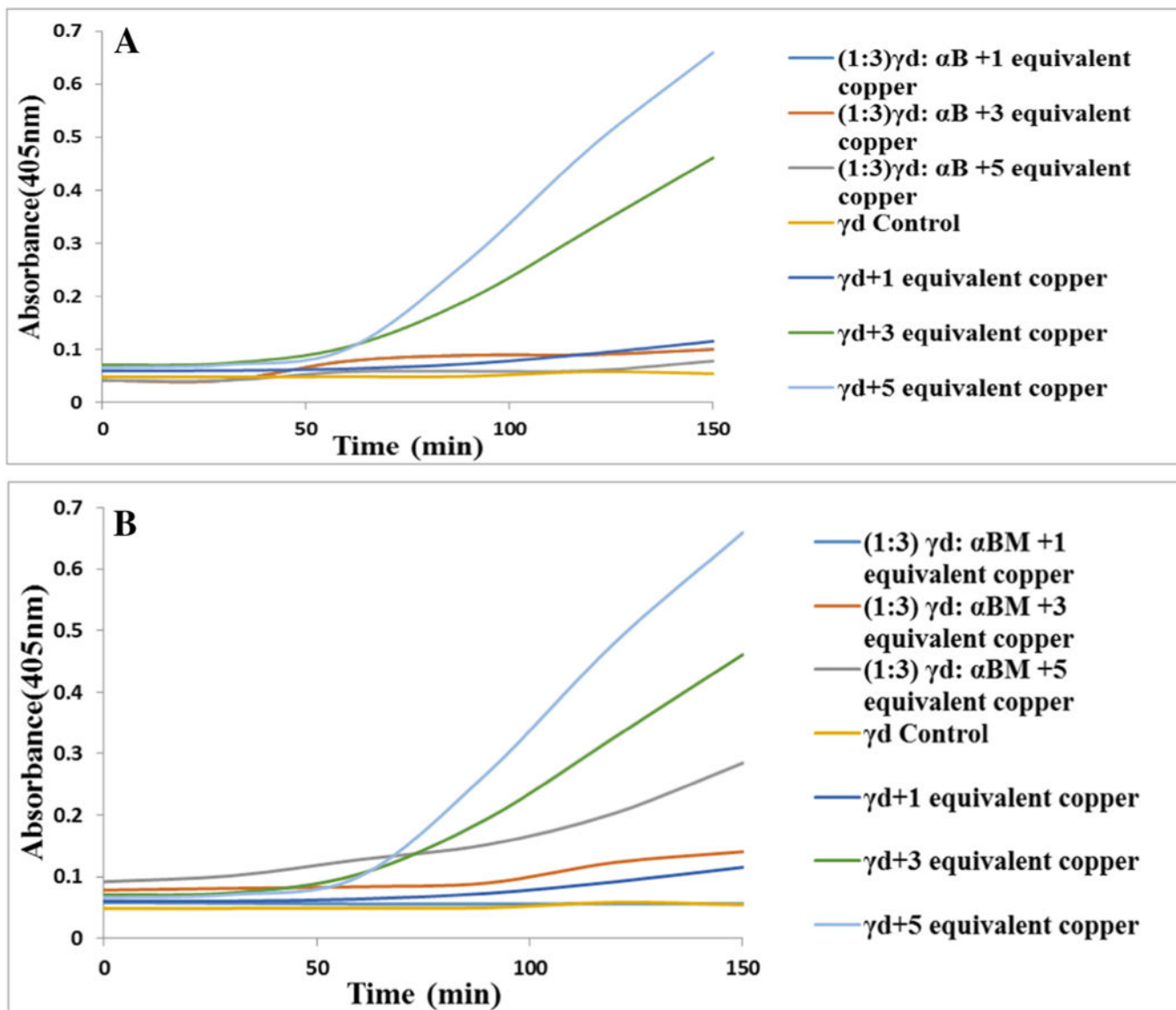




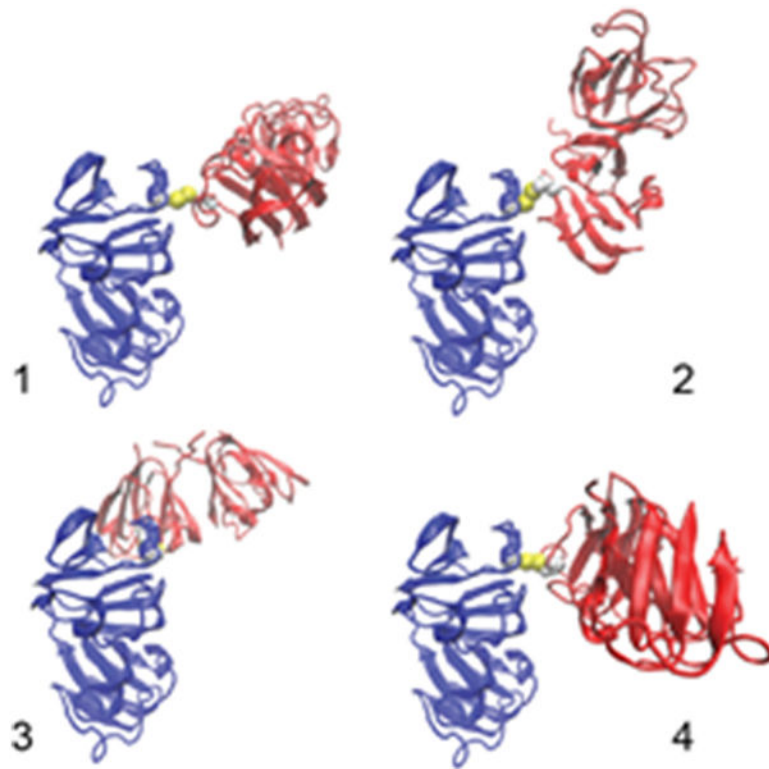
**Fig. 5.** Effect of Cu<sup>2+</sup> ions in the aggregation of hγD crystallin WT and cysteine mutants. (A) Turbidity assays of γD crystallin WT and single cysteine mutants (50 μM) in the absence or presence 1,3 and 5 equivalent of Cu<sup>2+</sup>. (B) Turbidity assays of γD crystallin WT and multiple cysteine mutant in the (50 μM) in the absence or presence of 1, 3, and 5 equiv. of Cu<sup>2+</sup>. In all experiments temperature was 37 °C, and the absorbance at 405 nm was measured 3 h after the addition of the metal ion. Turbidity assays were run six times ( $n = 6$ ) for each condition.



**Fig. 6.** Effect of  $\text{Cu}^{2+}$  ions in the aggregation of glutathionylated  $\gamma$ D crystallin WT. (A) Western Blot analysis of h $\gamma$ D incubated with GSSG using monoclonal GSH antibody. Antibody and the blot was developed using X-ray film using ECL solution the developed film was scanned under greyscale using Epson scanner 1:  $\gamma$ D crystallin WT alone, 2 & 3:  $\gamma$ D crystallin reacts with GSSG as indicated by the appearance of an immunoreactivity band. (B) Turbidity assays ( $n = 6$ ) of h $\gamma$ D crystallin, glutathionylated (Glu) h $\gamma$ D ( $50 \mu\text{M}$ ) incubated without or with 1, 3 and 5 equivalent of  $\text{Cu}^{2+}$  for 60 min.






**Fig. 7.** Effect of  $\alpha$ B crystallin and  $\alpha$ B crystallin minichaperone tested at 5 mg/ml on copper mediated aggregation of h $\gamma$ D crystallin. A:  $\alpha$ B crystallin totally suppressed aggregation. B:  $\alpha$ B minichaperone suppressed equally well except in presence of 5 equivalent  $\text{Cu}^{2+}$ .



**Fig. 8.**  
Top four dimeric models of human  $\gamma$ -D crystallin with intermolecular Cys111-Cys111.  
These models were ranked in order using the protein-protein docking software ClusPro [17].

Summary of recombinant hyD-crystallin cysteine sites (red color) in diamide oxidized hyD detected by LC-MS in tryptic digest of the monomer and dimer bands separated by SDS-PAGE.

**Table 1**

Crosslinked-peptide	Possible disulfide bridge	Mw (obs)	Mw	Mass error (ppm)	Monomer	Dimer
GQMIEFTDCSCLQ	C109-C111	1601.6277	1601.6282	0	X	X
DYRGMIEFTDCSCLQ	C109-C111	2035.8179	2035.8194	-1	X	X
	C19-C111	1447.4917	1447.4923	0	Very few	X
	C19-C111	2398.8957	2398.8931	1		X
	C111-C111	1718.6230	1718.6237	-1		X

**Table 2**

The disulfide bond by Cys111 of CRYGD in aged normal and cataractous human lenses (labeled by heavy ICAT) compared to young normal (labeled by light ICAT) from data that were manually extracted from mass spectra database [7].

ICAT lens type	Sample ID	Relative intensity		Ratio
		ICAT(0) light	ICAT(9) heavy	H/L
Aged normal	AN-1	21.27	100	4.7
	AN-2	n.d	n.d	n.d.
	AN-3	0	100	$\infty$
II cataract	Cat-II-1	12.9	100	7.7
	Cat-II-2	0	100	$\infty$
	Cat-II-3	9	100	11.1
III cataract	Cat-III-1	10	100	10.0
	Cat-III-2	0	100	$\infty$
	Cat-III-3	0	100	$\infty$
IV cataract	Cat-IV-1	0	100	$\infty$
	Cat-IV-2	0	100	$\infty$
	Cat-IV-3	0	100	$\infty$
V cataract	Cat-V-1	0	100	$\infty$
	Cat-V-2	0	100	$\infty$
	Cat-V-3	0	100	$\infty$